Supplemental Information Inventory

Supplemental Data (Five figures)

Figure S1. Targeted mutations of phosphorylation sites in stargazin. This figure contains information for generation and characterization of gene-targeting mice.

Figure S2. Stargazin phosphorylation increases AMPA receptor activity at synapses in cerebellar granule cells. Results using primary culture neurons, which are redundant with the figure 2 using acute brain slice. However, it is important to show similar results using different systems.

Figure S3. Stargazin binds specifically to AMPA receptors.

This result shows proteomic analysis for searching interactors with stargazin mutants

Figure S4. PSD-95 binding requires the four C-terminal-most amino acids of stargazin. This figure contains a diagram of new method we developed and control experiments.

Figure S5. The addition of sphingosine and squalamine, but not lipofectamine, induces dissociation of R-pre from the membranes. This figure contains control experiments.

Supplemental Experimental procedures

Experimental Procedures we previously published are moved from main text to here.

Supplemental Data

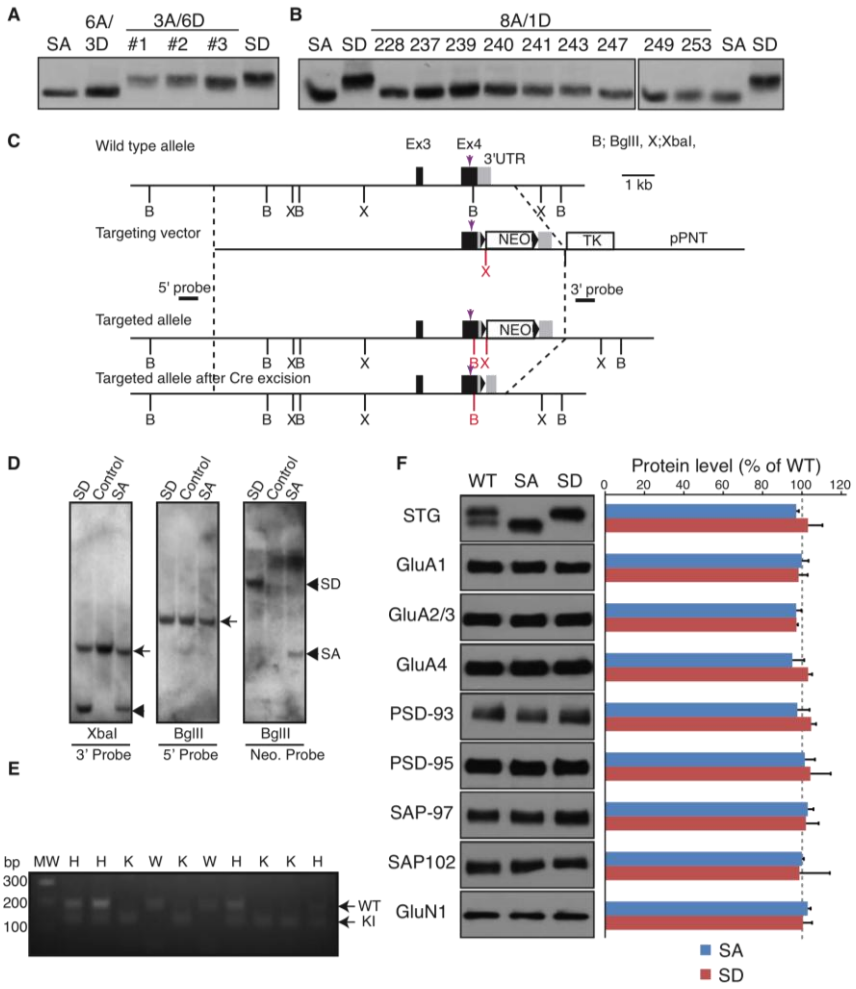

Figure S1. Targeted mutations of phosphorylation sites in stargazin. (A) The phosphomimic stargazin mutant (SD), which carried a substitution of the nine phosphorylatable serine residues in neurons with aspartate residues, exhibited graded shifts in mobility in a phosphomimic mutation-dependent manner (SA, 6A/3D, 3A/6D, and SD carried 0, 3, 6, and 9 aspartate mutations, respectively). Because endogenous stargazin at synapses co-migrated with stargazin^{SD} {Tomita, 2005 #92}, and stargazin^{SD} migrated at a higher molecular weight compared with 3A/6D, we concluded that synaptic stargazin was phosphorylated at more than six sites. Three different

combinations of 3A/6D were used (#1, #2, and #3). (B) No single mutation that substituted a serine to aspartate contributed to the mobility shifts observed for stargazin^{SD}. (C) Schematic representation of the stargazin protein, genomic locus, targeting vector, and targeted allele. Mutated phosphorylation sites were incorporated into the C-terminal cytoplasmic domain of stargazin by replacing wild-type exon 4 through homologous recombination. Lox P sites (black triangles) were used for Cre-recombinase removal of the neomycin cassette. (D) Southern blots of selected ES cell clones showed targeting of stargazin exon 4. A probe against the targeting vector 3' region yields a single fragment in wild-type cells (Control: arrow) and two fragments in heterozygous cells (arrow and arrowhead). A probe against the targeting vector 5' region yields a single fragment in both wild-type and heterozygous cells (arrows). A neomycin cassette probe yields no fragments in wild-type cells and a single fragment in heterozygous cells containing either phosphorylation-defective (SA) or constitutive phospho-mimic (SD) residues (arrowheads). The SD and SA mutations can be distinguished by Bgl II digests. (E) PCR genotyping of an individual mouse. W, wild type; H, heterozygous; K, homozygous knockins. (F) Expression of various synaptic proteins was quantitated in cerebella of wild-type (WT), stargazin^{SA}, and stargazin^{SD} mice. No significant differences in protein expression were detected among genotypes. Data are shown as means ± SEM (n = 4 cerebella).

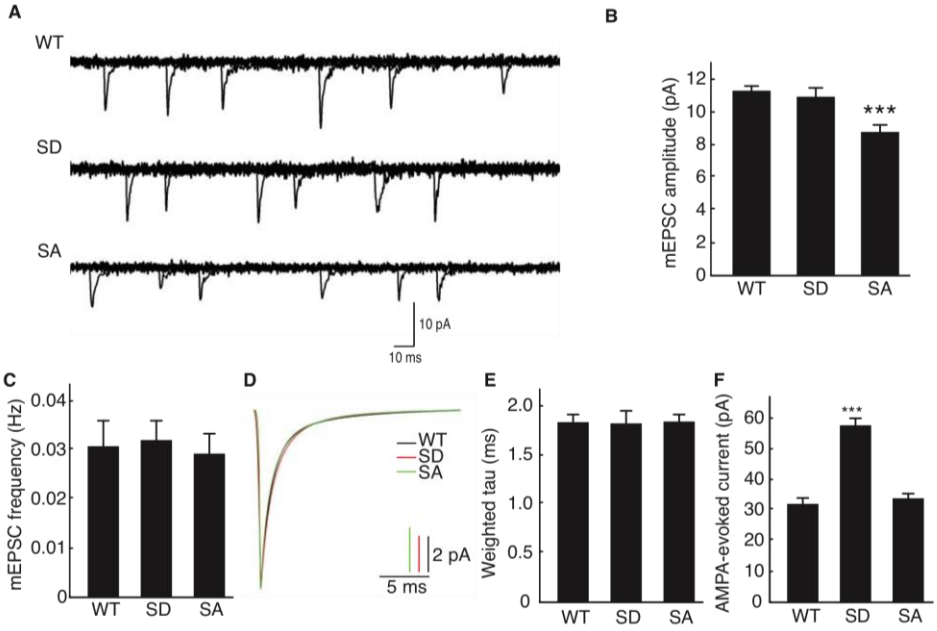

Figure S2. Stargazin phosphorylation increases AMPA receptor activity at synapses in cerebellar granule cells. (A-E) Synaptic AMPA receptor activity is higher in Stargazin^{SD} mice than Stargazin^{SA} mice. AMPA receptor-mediated miniature excitatory postsynaptic currents (mEPSCs) were recorded from cerebellar granule neurons. (A) Shown are representative AMPA receptor-mediated mEPSCs from each genotype. Mean amplitude (B) and frequency (C). (D, E) Decay kinetics were not significantly different among the genotypes. Weighted tau was calculated by fitting individual events to bi-exponential curves. (F) AMPA-evoked currents were significantly greater in neurons from Stargazin^{SD} mice than WT or Stargazin^{SA} mice, indicating that more AMPA receptors expressed at surface in Stargazin^{SD}. Whereas AMPA-evoked currents in WT and Stargazin^{SA} mice were at similar level, mEPSC amplitude in WT is larger than one in Stargazin^{SA}, indicating that Stargazin^{SA} expressed at the cell surface, but trapped outside of synapses. Data are shown as means ± s.e.m. (n = 160-180 events from 10-15 cells. Stargazin^{SD} (6 cells), stargazin^{SD} with GFP (5 cells),

stargazin^{SA} (5 cells), and stargazin^{SA} with GFP (5 cells), all results were mixed and analyzed). *** P<0.005.

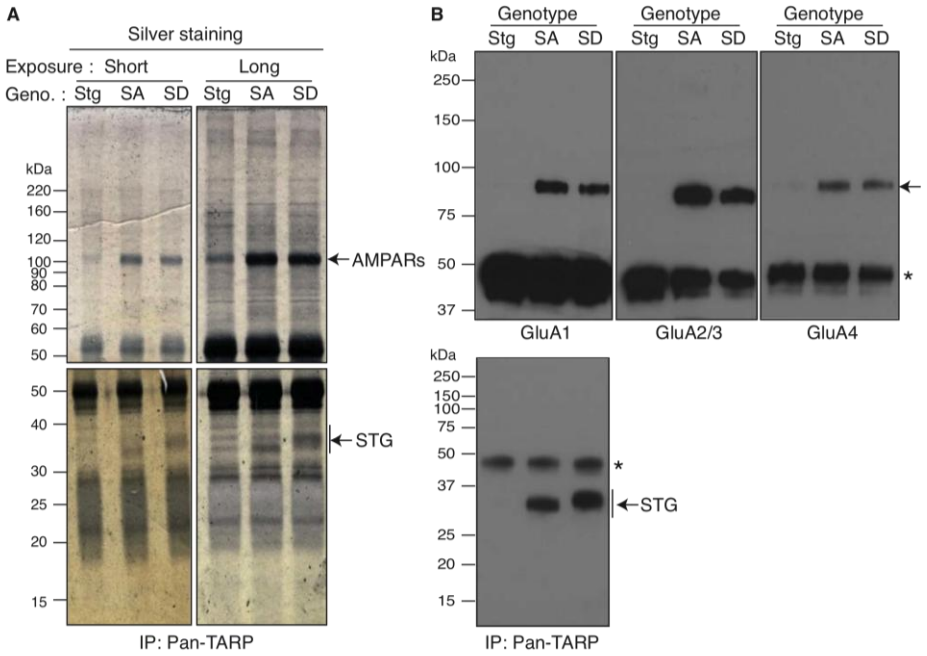

Figure S3. Stargazin binds specifically to AMPA receptors. (**A**) Cerebellar membranes were prepared from Stargazer (STG), Stargazin^{SD} (SD), and Stargazin^{SA} (SA) mice and then immunoprecipitated using anti-Pan-TARP antibody. Proteins eluted from protein A beads were separated by 6% (top) or 12% (bottom) SDS-PAGE. Silver staining of the 6% gel shows that a single band (~105 kDa) specifically co-immunoprecipitates with stargazin. (**B**) Western blotting confirms the precipitated band contains AMPAR subunits GluA1-4.

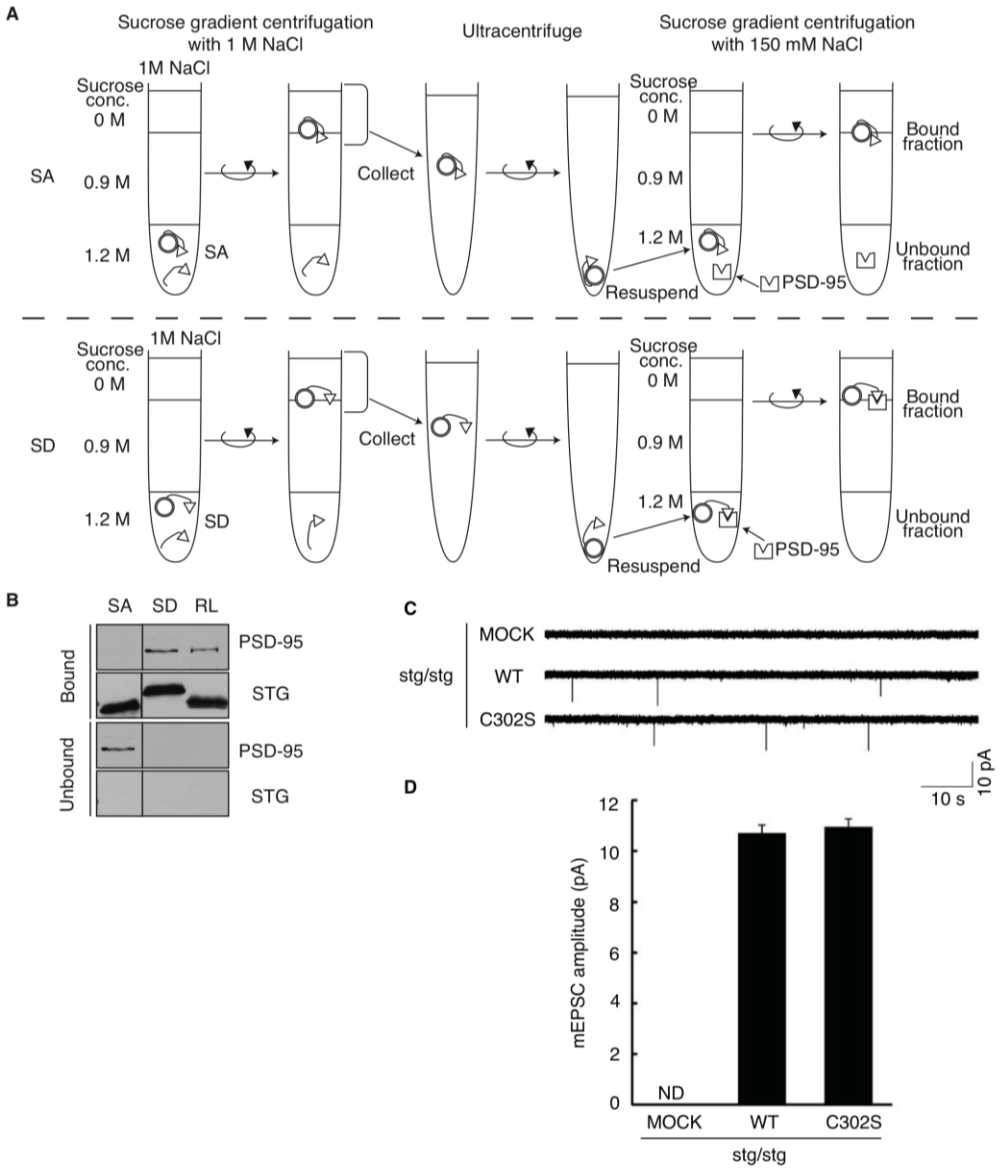

Figure S4. PSD-95 binding requires the four C-terminal-most amino acids of stargazin. (A) Schematic showing the experimental procedures for examining the effects of a lipid bilayer on stargazin-PSD-95 interactions. Liposomes (PC/PA/MPB-PE; 9:1:0.5) were prepared by freeze-thaw cycling and a mini-extruder with 100 nm polycarbonate membranes. 1, Liposomes containing MPB-PE were incubated with the cytoplasmic domain of stargazin, which contains a cysteine residue in its N terminus for thiol-maleimide link formation. 2, To separate unconjugated from liposome-conjugated proteins, sucrose gradient centrifugation was performed under high salt (1 M NaCl)

conditions, dissociating unconjugated stargazin from liposomes. 3, The top fraction containing stargazin-conjugated liposomes was collected and subjected to 100,000 g for 30 min. The liposome pellet was suspended in buffer containing 0.15 M NaCl. 4, Purified stargazin-conjugated liposomes were mixed with recombinant PDZ domains from PSD-95. 5, The mixture was adjusted to 1.2 M sucrose and separated by sucrose gradient centrifugation. Stargazin-bound PSD-95 was present in the top fraction and the unbound PSD-95 remained in the bottom fraction. (B) Liposomes containing MPB-PE were conjugated with the cytoplasmic domains of stargazin^{SA} (SA), stargazin^{SD} (SD), and stargazin^{RL} (RL), which was followed by examination of their interaction with the PDZ domain of PSD-95 using the floating assay described in Figure S4. The PDZ domain of PSD-95 bound liposomes conjugated with stargazin^{RL} and stargazin^{SD}, but not with stargazin^{SA}, indicating that interaction of stargazin with lipid bilayers suppresses stargazin binding to PSD-95. (C and D) A cysteine residue at position 302 in the cytoplasmic domain of stargazin is not involved in AMPA receptor activity at synapses. AMPA receptor-mediated miniature excitatory postsynaptic currents (mEPSCs) were recorded from cerebellar granule neurons. Cerebellar granule cells from *stargazer* mice were prepared and transfected with wild-type stargazin (WT) or with a stargazin mutant that carried a substitution of a cysteine residue at position 302 with a serine residue (C302S), to measure AMPAR mediated mEPSC. (C) Representative AMPA receptor-mediated mEPSCs from each genotype are shown. (D) The mean amplitudes were not significantly different between neurons transfected with WT and C302S. Data are shown as means ± SEM (n = 67 events from 10 WT-transfected cells and n = 72 events from 11 C302S-transfected cells).

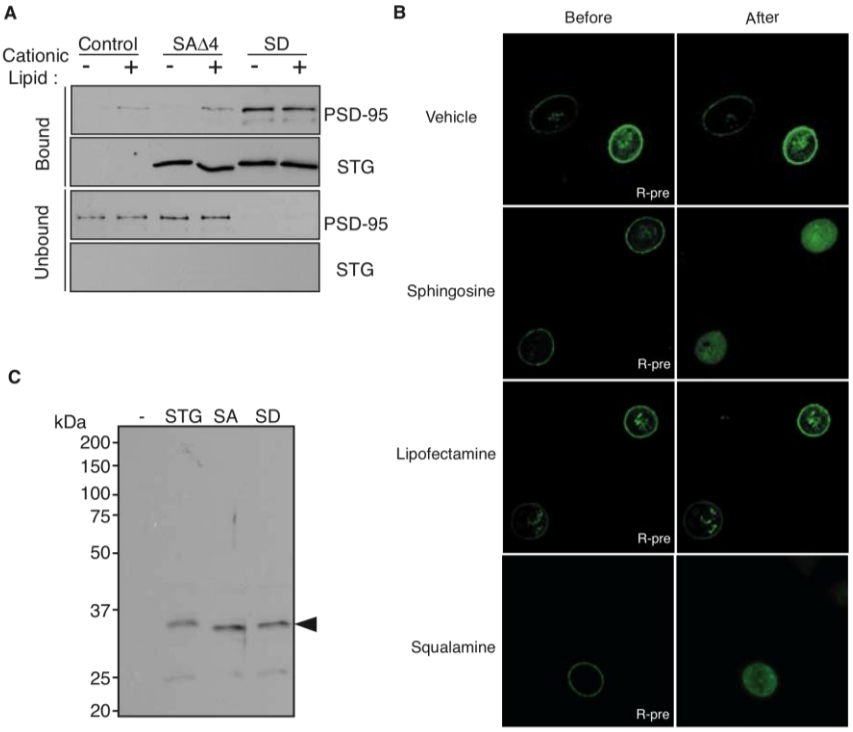

Figure S5. The addition of sphingosine and squalamine, but not lipofectamine, induces dissociation of R-pre from the membranes. (A) Liposomes containing MPB-PE were conjugated with cysteine (control), the cytoplasmic domain of stargazin^{SA} lacking the last four amino acids (SAΔ4), and stargazin^{SD} (SD). Addition of lipofectamine (Cationic lipid) increased PSD-95 binding to SAΔ4, to an extent that was similar to that of liposomes conjugated with cysteine alone, which suggests that the weak signal observed was non-specific. (B) CHO cells were transfected with GFP-tagged R-Pre, which interacts with negatively-charged membranes. Addition of the cationic lipids, sphingosine and squalamine, induced re-localization of GFP-tagged R-pre from the plasma membrane to the cytosol, whereas addition of vehicle (ethanol) or the cationic lipid lipofectamine did not. This result suggests that lipofectamine does not incorporate into inner leaflet of plasma membranes. (C) Expression of the cytoplasmic domains of stargazin mutants tagged with GFP and a myristoylation motif. A myristoylation motif and a GFP moiety were tagged to the N terminus and C terminus,

respectively, of the cytoplasmic domains of wild-type stargazin (STG), stargazin^{SA} (SA), and stargazin^{SD} (SD), which was followed by their expression in CHO cells. The molecular weights were confirmed as being similar to the expected values. Importantly, wild-type stargazin migrated at a size that was similar to that of SD, which indicates that wild-type stargazin was phosphorylated in CHO cells.

Supplemental Experimental Procedures

Stargazin gene-targeting in the mouse

The stargazin gene comprises of 4 exons. We designed a targeting vector that replaced exon 4, which encodes the C-terminal cytoplasmic domain, with a mutated exon 4 (non-phospho-mimic, stargazin^{SA}; phospho-mimic, stargazin^{SD}). Exon 4 was inserted with a Lox P-flanked neomycin resistant gene, allowing the neomycin cassette to be removed after germline transmission. The targeting construct was electroporated into embryonic stem (ES) cells and, following double-drug selection, surviving cell colonies were picked and expanded. Southern blots were used to confirm proper homologous recombination. ES cells were injected into mouse blastocysts by the Yale University Transgenic Mouse Service. Chimeric mice were identified by coat color and mated to Actin-Cre mice. Heterozygous male and female mice were subsequently mated to obtain homozygous knockin mice. In addition, these mice were crossed with Actin-GFP mice purchased from Jackson Laboratory to obtain homozygous knockin mice carrying the GFP transgene so that genotypes could be visually identified. All mice were maintained at the Yale animal facility under the guidelines of the Institutional Animal Care and Use Committee.

Whole cell recording from cerebellar granule cells

All mice were maintained at the Yale animal facility under the guidelines of the Institutional Animal Care and Use Committee. Cerebellar granule cell cultures were prepared from postnatal day 7 (P7) homozygous knockin mice and homozygous knockins carrying the additional GFP transgene, as described previously (Zhang et al.,

2009). Patch clamp recordings from cerebellar granule cells (DIV8-11) were performed in external solution containing (in mM): 10 HEPES, 140 NaCl, 2.5 KCl, 2.5 $CaCl_2$, 1.3 $MgSO_4$, 2.7 $MgCl_2$, and 10 glucose. Patch pipettes were filled with recording solution (pH 7.2) that contained (in mM): 130 caesium methanesulfonate, 5 HEPES, 5 Mg-ATP, 0.2 Na-GTP, 20 TEA, and 5 EGTA. All recordings were performed at room temperature. To isolate and record the AMPA receptor-mediated mEPSCs, tetrodotoxin (1 µM), AP-5 (100 µM) and picrotoxin (100 µM) were added to the external solution. The mEPSCs were recorded from cerebellar granule cells in the whole-cell configuration, at a holding potential of -70 mV. The current was analogue low-pass filtered at 3 kHz and sampled digitally at 25 kHz. Amplitude and frequency of events were analyzed using Minianalysis (Synaptosoft) and the detection threshold was set to 5 pA. From each cell analyzed, 15 to 20 randomly picked mEPSCs were fitted with bi-exponential functions to determine decay kinetics (tau). Both T-test and ANOVA followed by Tukey's test were used; cumulative distribution was compared by Kolmogorov-Smirnov test.

Co-immunoprecipitation of stargazin with PSD-95

Solubilization of PSD-95 from neurons requires the use of a strong detergent, such as 1% SDS, which breaks the interaction of PSD-95 with stargazin. Therefore, we used a chemical crosslinker to detect the interaction of PSD-95 with stargazin. Cerebellar granule cells were treated with the DSP crosslinker (20 µM) for 10 min at 4° C, which was followed by lysis with 1% SDS. After brief sonication, lysates were neutralized with a buffer containing 1% Triton X-100, for immunoprecipitation. Solubilized proteins were subjected to immunoprecipitation using an anti-stargazin antibody (STG).

To avoid artificial interaction between stargazin and PSD-95 during incubation, we added 100 μM of a stargazin C-terminal 10-mer peptide (NTANRRTTPV) to detect crosslinked complexes exclusively *in vivo*.

Immunoprecipitation

Mouse cerebellar membranes were suspended in lysis buffer (20 mM Tris-Cl [pH 8.0], 2 mM EDTA, 1 mM DTT), 1% Triton X-100 and protease inhibitors (1 mM PMSF, 10 μg/ml leupeptin) and were centrifuged at 100,000 g for 1 h. Pre-cleared supernatants were then incubated with 3 μg of affinity-purified antibodies and 20 μl of protein A sepharose beads. Bound proteins were eluted with 1X SDS-PAGE sample buffer and separated by SDS-PAGE, followed by silver staining and western blotting.

Purification of recombinant proteins

The cytoplasmic domain of stargazin (amino acids 203-323) was tagged with either GST or His6-thioredoxin, and the PSD-95 PDZ domains (amino acids 62-402) were tagged with GST. Recombinant proteins were expressed in *Escherichia coli* and GST fusion proteins were purified with glutathione-sepharose, as described previously (Dakoji et al., 2003).

In vitro binding assays with GST fusion proteins

GST fusion proteins were loaded onto glutathione-sepharose beads (GE Healthcare) and incubated with the stargazin cytoplasmic domain at 4°C. The beads were washed extensively with washing buffer containing 1% Triton X-100. Proteins retained on the

beads (bound fraction), and those that did not bind, were resolved further by SDS-PAGE analysis and visualized by western blotting.

Fractionation of cerebellar granule cells

Cerebellar granule cells (DIV14) were treated with 10 μM sphingosine or vehicle (ethanol) for 5 min. The cells were then lysed with the lysis buffer (20 mM Tris-Cl [pH 7.6], 150 mM NaCl, 5 mM EDTA, 1 mM EGTA, 1% Triton X-100). Solublized proteins were then collected as the Triton X-100 solubilized fraction (Syn/Tx). The pellets were then solubilized with 1X SDS-PAGE sample buffer as the PSD fraction (PSD).